

# Quadratic Hyperpolarizability of Carbomeric Structures

Jean-Marie Ducere,<sup>†</sup> Christine Lepetit,<sup>†</sup> Pascal G. Lacroix,<sup>†</sup>  
Jean-Louis Heully,<sup>‡</sup> and Remi Chauvin<sup>\*,†</sup>

Laboratoire de Chimie de Coordination, UPR 8241 CNRS, 205 Route de Narbonne,  
31077 Toulouse Cedex 4, France, and Laboratoire de Physique Quantique, UMR 5626 CNRS,  
118 route de Narbonne, 31062 Toulouse, France

Received December 10, 2001. Revised Manuscript Received May 14, 2002

The ZINDO-computed quadratic hyperpolarizability ( $\beta$ ) of *p*-nitroaniline (PNA) is compared with that of its carbomer in its molecular mechanics (MM) optimized geometry. Complete carbomerization of PNA leads to a new molecule with a static  $\beta_0$  value of  $941.3 \times 10^{-30} \text{ cm}^5 \text{ esu}^{-1}$  which is 2 orders of magnitude better than that of PNA. Within the model of push–pull molecular topography, an empirical five-parameter formula is proposed in order to estimate the  $\beta$  value of 32 partial carbomer structures of *p*-nitroaniline. A compromise between high  $\beta$  values and a priori synthetic feasibility is achieved for structures with three carbomerized domains only: the carbon skeleton of the *p*-phenylene ring, the nitro group, and the phenylene–nitro bond. The results are discussed within the framework of the two-level model on the basis of an orbital analysis. A relevant measure of the molecular NLO response is proposed to be the “specific quadratic hyperpolarizability”:  $[\beta] = \beta/N$ , where  $N$  is the number of non-hydrogen atoms in the molecule. This quantity applies to all kinds of molecular topology and is fundamentally related to the volumic bulk material NLO efficiency  $\chi^{(2)}$ . According to this measure, the size-normalized effect of the carbomerization process (size expansion + symmetry preservation) is a 30 time enhancement of  $[\beta]$  at the level of theory used. The carbomerization process is generalized to several donors ( $\text{NH}_2$ ,  $\text{CH}_3$ , Ph, ...) and conjugated links (*p*- $\text{C}_6\text{H}_4$ , *trans*- $\text{CH}=\text{CH}$ ,  $\text{C}\equiv\text{C}$ ) in push–pull chromophores. The MM-optimized structure of *p*-[C,C]<sub>6</sub>carbophenyl-[CC]<sub>7</sub>[NC]<sub>2</sub>[CO]<sub>2</sub>carbo-nitrobenzene has a  $\beta$  value of 200 times that of *p*-nitroaniline. In all instance, the very strong withdrawing effect of the carbonitro group is pointed out. This intriguing substituent, which up to now has never been reported either experimentally or theoretically, is thoroughly investigated at various levels including DFT, MP2, QCISD, and CASSCF.

## Introduction

The carbomer structure of any given molecule is the molecular structure obtained by inserting a dicarbon  $\text{C}_2$  unit into each bond of the representative Lewis structure of the original structure.<sup>1</sup> By applying a basic Lewis electron count and VSEPR theory, it is readily seen that any molecule and its carbomeric equivalent in their respective equilibrium state should have grossly (i) the same symmetry, (ii) the same shape of the nuclear vertice geometry, and (iii) the same resonance properties. The proposition of this general formalism proved to be useful as it naturally triggered the drawing of novel putative chemical structures which became synthetic targets owing to their esthetics and obvious potential physicochemical properties.<sup>2</sup> Moreover, the questions of how properties are preserved or systematically transferred through the “carbomerization” process is naturally addressed. It has been shown by DFT and ab initio calculations that aromaticity and antiaroma-

ticity are preserved upon carbomerization: the carbomer of an (anti)aromatic structure is indeed (anti)aromatic in the structural, magnetic, and energetic senses.<sup>3</sup> In the search for other preservation or systematic transposition laws between carbomeric partners (“carbomeric comparisons”), the importance of nonlinear optical phenomena in modern material sciences prompted us to investigate the effect of carbomerization on the quadratic hyperpolarizability tensor ( $\beta$ ). Many one-dimensional charge-transfer organic systems with sizable  $\beta$  values have been investigated since the mid 1970s.<sup>4</sup> The typical benchmark molecule is *p*-nitroaniline (PNA, **1a**; Scheme 1), a chromophore which has served as a model compound for many investigations.<sup>5</sup> Attempts to further increase the nonlinearity were aimed at increasing the length of the conjugation bridge between donor and acceptor ends.<sup>6</sup> Another strategy

(3) Godard, C.; Lepetit, C.; Chauvin, R. *Chem. Commun.* **2000**, 1833.

(4) (a) *Nonlinear Optical Properties of Organic Molecules and Crystals*; Chemla, D. S., Zyss, J., Eds.; Academic Press: New York, 1987; Vols. 1 and 2. (b) *Molecular Nonlinear Optics*; Zyss, J., Ed.; Academic Press: New York, 1994. (c) *Nonlinear Optics of Organic Molecules and Polymers*; Nalwa, H. S., Miyata, S., Eds.; CRC Press: Boca Raton, FL, 1997.

(5) Williams, D. J. *Angew. Chem., Int. Ed. Engl.* **1984**, 23, 690.

(6) (a) Oudar, J. L. *J. Chem. Phys.* **1977**, 67, 446. (b) Oudar, J. L.; Chemla, D. S. *J. Chem. Phys.* **1977**, 66, 2664.

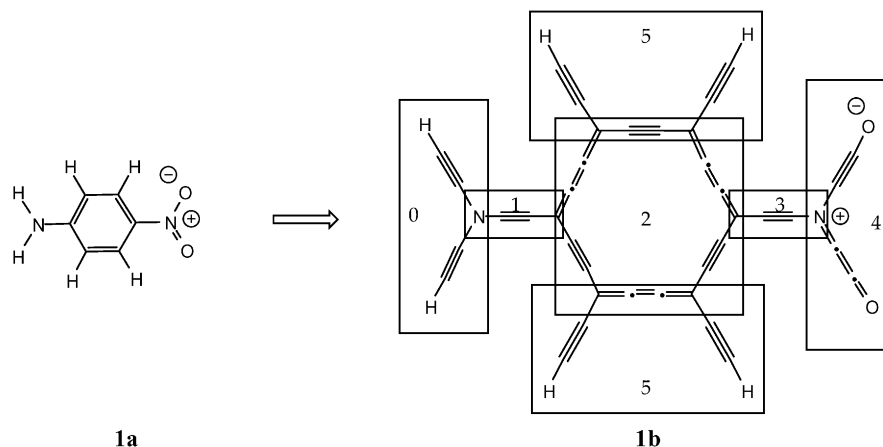
\* To whom correspondence should be addressed. Phone: 05 61 33 31 13. Fax: 05 61 55 30 03. E-mail: chauvin@lcc-toulouse.fr.

<sup>†</sup> Laboratoire de Chimie de Coordination, UPR 8241 CNRS.

<sup>‡</sup> Laboratoire de Physique Quantique, UMR 5626 CNRS.

(1) Chauvin, R. *Tetrahedron Lett.* **1995**, 36, 397.

(2) Maurette, L.; Godard, C.; Frau, S.; Lepetit, C.; Soleilhavoup, M.; Chauvin, R. *Chem. Eur. J.* **2000**, 7, 1165.

Scheme 1. *p*-Nitroaniline and Its Carbomer

implies increasing the donor and acceptor strength in a given conjugated bridge.<sup>7</sup> In the early 1990s, Marder et al. proposed an alternative approach for the optimization of a chromophore.<sup>8</sup> In striking contrast to the previous approaches, they showed that, for a given conjugated bridge, there is an optimal combination of donor and acceptor strength which maximizes  $\beta$ : beyond this point, increasing the donor–acceptor strength of the substituents leads to  $\beta$  attenuation. These observations suggest that optimizing the donor, the acceptor, and the conjugated bridge should no longer be achieved independently and would benefit from a global approach of the molecule. Along this line, the carbomerization appears attractive as it is expected to increase the scale of a chromophore, and hence the  $\beta$  value, without qualitatively affecting the electronic features, once they have been optimized in a reference molecule such as **1a**.

The present contribution addresses the carbomeric comparison of the vectorial hyperpolarizability coefficient  $\beta$  of the *p*-nitroaniline **1a**, which has been the first optimized “push–pull” organic chromophore thoroughly investigated as a NLO chromophore.

## Computational Details

The geometry of the 32 partial or complete carbomer structures of *p*-nitroaniline were calculated by molecular mechanics (MM) using the CVFF force field of Discover.<sup>9</sup> Because this force field is not able to reproduce the aromatic character of the *p*-carbophenylene ring (observed experimentally,<sup>10</sup> and reproduced by DFT calculations at the B3PW91/6-31G\*\* level),<sup>11</sup> the geometry of this ring was extracted from DFT calculations, and a  $C_{2v}$  symmetry constraint has been enforced during geometry optimization.

Geometry optimizations and vibrational analysis of  $\text{HNC}_4\text{O}_2$  were performed at various levels using Gaussian 94/98<sup>12</sup> or NWChem.<sup>13</sup> The multiconfigurational calculations were performed with MOLCAS.<sup>14</sup>

The all-valence INDO (intermediate neglect of differential overlap) method,<sup>15</sup> in connection with the sum-over-state (SOS) formalism,<sup>16</sup> was employed for the calculation of the molecular hyperpolarizabilities. Details of the computationally efficient INDO–SOS-based method for describing second-order molecular optical nonlinearities have been reported elsewhere.<sup>17</sup> Calculations were performed using the INDO/1 Hamiltonian incorporated in the commercially available MSI software package ZINDO.<sup>18</sup> The monoexcited configuration interaction (MECI) approximation was employed to describe the excited states. The 300 lowest energy one-electron transitions between the 20 highest occupied molecular orbitals and the 20 lowest unoccupied ones

(7) (a) Cheng, L. T.; Tam, W.; Stevenson, S. H.; Meredith, G. R.; Rikken, G.; Marder, S. R. *J. Phys. Chem.* **1991**, *95*, 10631. (b) Cheng, L. T.; Tam, W.; Marder, S. R.; Stiegman, A. E.; Rikken, G.; Spangler, C. W. *J. Phys. Chem.* **1991**, *95*, 10643.

(8) (a) Marder, S. R.; Beratan, D. N.; Cheng, L.-T. *Science* **1991**, *252*, 103. (b) Marder, S. R.; Gorman, C. B.; Tieman, B. G.; Cheng, L.-T. *J. Am. Chem. Soc.* **1993**, *115*, 3006.

(9) Discover, release 95.0; Biosym Technologies: San Diego, CA, 1996.

(10) (a) Suzuki, R.; Tsukuda, H.; Watanabe, N.; Kuwatani, Y.; Ueda, I. *Tetrahedron* **1998**, *54*, 2477. (b) Chauvin, R. *Tetrahedron Lett.* **1995**, *36*, 401.

(11) Lepetit, C.; Godard, C.; Chauvin, R. *New J. Chem.* **2001**, *25*, 572.

(12) (a) Frisch, M. J.; Trucks, G. W.; Schlegel, H. B.; Gill, P. M. W.; Johnson, B. G.; Robb, M. A.; Cheeseman, J. R.; Keith, T.; Petersson, G. A.; Montgomery, J. A.; Raghavachari, K.; Al-Laham, M. A.; Zakrzewski, V. G.; Ortiz, J. V.; Foresman, J. B.; Cioslowski, J.; Stefanov, B. B.; Nanayakkara, A.; Challacombe, M.; Peng, C. Y.; Ayala, P. Y.; Chen, W.; Wong, M. W.; Andres, J. L.; Replogle, E. S.; Gomperts, R.; Martin, R. L.; Fox, D. J.; Binkley, J. S.; Defrees, D. J.; Baker, J.; Stewart, J. P.; Head-Gordon, M.; Gonzalez, C.; Pople, J. A. *Gaussian 94*, revision E.2; Gaussian, Inc.: Pittsburgh, PA, 1995. (b) Frisch, M. J.; Trucks, G. W.; Schlegel, H. B.; Scuseria, G. E.; Robb, M. A.; Cheeseman, J. R.; Zakrzewski, V. G.; Montgomery, J. A., Jr.; Stratmann, R. E.; Burant, J. C.; Dapprich, S.; Millam, J. M.; Daniels, A. D.; Kudin, K. N.; Strain, M. C.; Farkas, O.; Tomasi, J.; Barone, V.; Cossi, M.; Cammi, R.; Mennucci, B.; Pomelli, C.; Adamo, C.; Clifford, S.; Ochterski, J.; Petersson, G. A.; Ayala, P. Y.; Cui, Q.; Morokuma, K.; Malick, D. K.; Rabuck, A. D.; Raghavachari, K.; Foresman, J. B.; Cioslowski, J.; Ortiz, J. V.; Stefanov, B. B.; Liu, G.; Liashenko, A.; Piskorz, P.; Komaromi, I.; Gomperts, R.; Martin, R. L.; Fox, D. J.; Keith, T.; Al-Laham, M. A.; Peng, C. Y.; Nanayakkara, A.; Gonzalez, C.; Challacombe, M.; Gill, P. M. W.; Johnson, B. G.; Chen, W.; Wong, M. W.; Andres, J. L.; Head-Gordon, M.; Replogle, E. S.; Pople, J. A. *Gaussian 98*, revision A.7; Gaussian, Inc.: Pittsburgh, PA, 1998.

(13) NWChem 3.3; Pacific Northwest National Laboratory: Richland, WA, 1999.

(14) Anderson, K.; Blomberg, M. R. A.; Fulscher, M. P.; Karlstrom, G.; Lindh, R.; Malmqvist, P.-A.; Neogrady, P.; Olsen, J.; Roos, B. O.; Sadlej, M.; Schutz, A. J.; Seijo, L.; Serrano-Andres, L.; Siegbahn, P. E. M. P. O. *Molcas4 Program Package*, Widmark, Lund University: Lund, Sweden 1997.

(15) (a) Zerner, M. C.; Loew, G.; Kirchner, R.; Mueller-Westerhoff, U. *J. Am. Chem. Soc.* **1980**, *102*, 589. (b) Anderson, W. P.; Edwards, D.; Zerner, M. C. *Inorg. Chem.* **1986**, *25*, 2728.

(16) Ward, J. F. *Rev. Mod. Phys.* **1965**, *37*, 1.

(17) Kanis, D. R.; Ratner, M. A.; Marks, T. J. *Chem. Rev.* **1994**, *94*, 195.

(18) ZINDO, 96.0/4.0.0; Molecular Simulations Inc.: Cambridge, U.K., 1996.

were chosen to undergo CI mixing. It was checked to be sufficient for reaching  $\beta$  convergence.

### General Results

The simplest structural scheme inspiring the design of highly hyperpolarizable organic molecular structures, consists of an oriented sequence of (i) a  $\pi$ -donating function, (ii) a bond, (iii) a bridge, (iv) a bond, and (v) a  $\pi$ -accepting function, plus (vi) a branched bystanding domain where chiral functions could be anchored in order to prevent condensation in centrosymmetric materials.

Within the framework of the SOS perturbation theory,  $\beta$  can be related to all excited states ( $j$ ) of a molecule and can be partitioned into two contributions, so-called  $\beta_{2\text{level}}$  and  $\beta_{3\text{level}}$ . Analysis of term contributions to the hyperpolarizability of push–pull organics indicates that  $\beta_{2\text{level}}$  dominates the nonlinearity. Therefore, the simplified expression of  $\beta$  is the following:

$$\beta \approx \beta_{2\text{level}} = \sum_i \frac{3e^2 \hbar f_i (\Delta\mu)_i}{2m(\Delta E)_i^3 ((\Delta E)_i^2 - (2\hbar\omega)^2)((\Delta E)_i^2 - (\hbar\omega)^2)} (\Delta E)_i^4 \quad (1)$$

with  $(\Delta E)_i$  being the energy gap between the  $i$ th excited state and the ground state,  $\Delta\mu_i$  being the corresponding variation of the electric dipole moment, and  $f_i$  being the oscillator strength of the transition.  $\hbar\omega$  is the energy of the laser beam. In eq 1, the summation is run over all of the transitions of the molecule. However, a single (usually HOMO  $\rightarrow$  LUMO based) transition is frequently responsible for most of the nonlinearity of push–pull organics (two-level model).<sup>19</sup> In eq 1, the expression indicates that when  $\hbar\omega$  is close to  $\Delta E_1 = \Delta E$  the dispersion factor  $(\Delta E)_i^4 / ((\Delta E)_i^2 - (2\hbar\omega)^2)((\Delta E)_i^2 - (\hbar\omega)^2)$  is artificially enhanced by resonance. Therefore, it is more relevant to consider the static hyperpolarizability ( $\beta_0$ ), which is independent of the laser beam frequency and, therefore, reveals the intrinsic nonlinearity of the molecule. This leads to the simplified relation:

$$\beta_0 = \frac{3e^2 \hbar}{2m} \frac{f \Delta\mu}{(\Delta E)^3} \quad (2)$$

The carbomer of a push–pull structure is a push–pull structure as well, thus preserving the requirement for the approximation of eq 2.<sup>20</sup> Furthermore, the  $\beta_0$  value is anticipated to be increased in carbomeric structure because  $\pi_z$ -type HOMO–LUMO gaps should be smaller in more conjugated molecules.<sup>3</sup>

The calculated static and frequency-dependent hyperpolarizability of planar  $C_{2v}$  structures of **1a** and **1b** (Scheme 1) derived from MM optimization ( $\beta_0(\mathbf{1a}) = 10.1 \times 10^{-30} \text{ cm}^5 \text{ esu}^{-1}$ ,  $\beta(\lambda = 1064 \text{ nm})(\mathbf{1a}) = 19.9 \times 10^{-30} \text{ cm}^5 \text{ esu}^{-1}$ , and  $\beta_0(\mathbf{1b}) = 941.3 \times 10^{-30} \text{ cm}^5 \text{ esu}^{-1}$ ), may be compared with the experimental  $\beta(\lambda = 1064 \text{ nm})(\mathbf{1a})$  value equal to  $34.5 \times 10^{-30} \text{ cm}^5 \text{ esu}^{-1}$ .<sup>19</sup> The reliability of our methodology in the prediction of the  $\beta$

**Table 1. Calculated Hyperpolarizability  $\beta(\lambda = \infty)$  and Specific Hyperpolarizability  $[\beta] = \beta/N$  of 16 Partial Carbomers  $\epsilon_1\epsilon_2\epsilon_3\epsilon_4$  of PNA 1a in  $10^{-30} \text{ cm}^5 \text{ esu}^{-1}$  Units**

$\epsilon_1\epsilon_2\epsilon_3\epsilon_4$	$\beta^a$	$\beta_{2\text{level}}^b$	$\mu^c$	$\mu\beta$	$N^d$	$[\beta]$	$[\beta]\mu$
0000	<b>(1a)</b> 10.12	15.99	8.79	88.97	10	1.01	8.90
0001	26.79	54.36	12.81	343.18	14	1.91	24.47
0010	25.15	34.93	10.03	252.25	12	2.10	21.06
0011	87.85	139.60	13.41	1177.97	16	5.49	73.63
0100	23.09	102.69	14.94	343.96	22	1.05	15.69
0101	97.33	274.37	26.38	2567.57	26	3.74	98.66
0110	85.12	179.49	15.95	1357.72	24	3.55	56.57
0111	<b>(1c)</b> 809.9	1347.43	22.84	18498.88	28	28.93	660.7
1000	18.80	31.93	9.05	170.14	12	1.57	14.21
1001	52.03	94.29	13.07	680.03	16	3.25	42.48
1010	34.73	54.87	10.01	347.65	14	2.48	24.82
1011	112.45	191.48	13.36	1502.33	18	6.25	83.50
1100	56.03	160.81	14.72	824.76	24	2.33	34.30
1101	407.28	683.21	22.56	9188.23	28	14.55	328.25
1110	135.76	261.04	15.28	2074.41	26	5.22	79.76
1111	967.01	1571.27	21.91	21187.19	30	32.23	706.16
	<b>(1b)</b> 941.28	1347.62	18.24	17168.95	42	22.41	408.76

<sup>a</sup>  $\beta = \beta_{2\text{level}} + \beta_{3\text{level}}$ . <sup>b</sup>  $\beta_{2\text{level}}$  is defined in eq 1. <sup>c</sup> Debye units. <sup>d</sup>  $N$  denotes the number of non-hydrogen atoms of the structure.

magnitude is found to be satisfactory. Complete carbomerization leads to a  $\beta$  value about 100 times higher than the  $\beta$  value of the parent molecule. To avoid undesirable  $\beta$  enhancements because of resonance effects and, therefore, to make better comparisons, any calculated hyperpolarizabilities will be the static  $\beta_0$  in the next sections. For the sake of simplification, these hyperpolarizabilities will simply be labeled  $\beta$ .

Within the prospect of an experimental synthesis of carbomer-derived molecules exhibiting a high  $\beta$ , it is important to identify unessential bond carbomerization. Partial carbomerization must however preserve the gross (VSEPR-predicted) symmetry of **1a**. On Scheme 2, six symmetry-adapted carbomerization domains are defined:  $2^6 = 64$  structures are thus constructed and characterized by sets of six digits  $\epsilon_0\epsilon_1\epsilon_2\epsilon_3\epsilon_4\epsilon_5$  where  $\epsilon_i = 1$  when the domain  $i$  is carbomerized and  $\epsilon_i = 0$  otherwise. Structure **1a** and **1b** are thus denoted as 000000 and 111111, respectively. However, preliminary calculations have shown that (i) the carbomerization of the four lateral C–H bonds of the *p*-phenylene ring should have a negligible influence on the  $\beta$  value (the size expansion is indeed perpendicular to the charge-transfer axis: see below) and (ii) the donating ability of the donor group  $\text{NR}_2$  is strictly located at the nitrogen atom, where the conjugated  $\pi$  system stops, and carbomerization of the N–H bonds has a negligible influence as well. Structures with noncarbomerized N–H bonds (domain 0) and C–H bonds (domain 5), will be therefore denoted by a four-digit description,  $\epsilon_1\epsilon_2\epsilon_3\epsilon_4$  (implicitly:  $\epsilon_0 = \epsilon_5 = 0$ ).

The calculated  $\beta$  values of the corresponding 16 structures  $\epsilon_1\epsilon_2\epsilon_3\epsilon_4$  lie in the range  $10\text{--}967 \times 10^{-30} \text{ cm}^5 \text{ esu}^{-1}$  (Table 1). The latter outstanding values deserve a further analysis of the carbomerization effect. For a given domain  $i$  of the molecular topology (Scheme 1), and whatever the configurations (carbomerized or not) of the remaining domains, the calculated  $\beta$  values of  $i$ -carbomerized structures are plotted versus those of the non- $i$ -carbomerized ones. For each domain, one obtains an accurate linear fit passing through the origin (Figure 1): indeed, carbomerization of structures having a zero  $\beta$  value should have a zero  $\beta$  value as well. One-parameter linear regressions afford slope values  $m_i$  for

(19) Oudar, J. L.; Chemla, J. J. *Chem. Phys.* **1977**, *66*, 2664.

(20) The relative weights of the resonance forms in the ground state and excited states should a priori have the same order of magnitude in both structures.



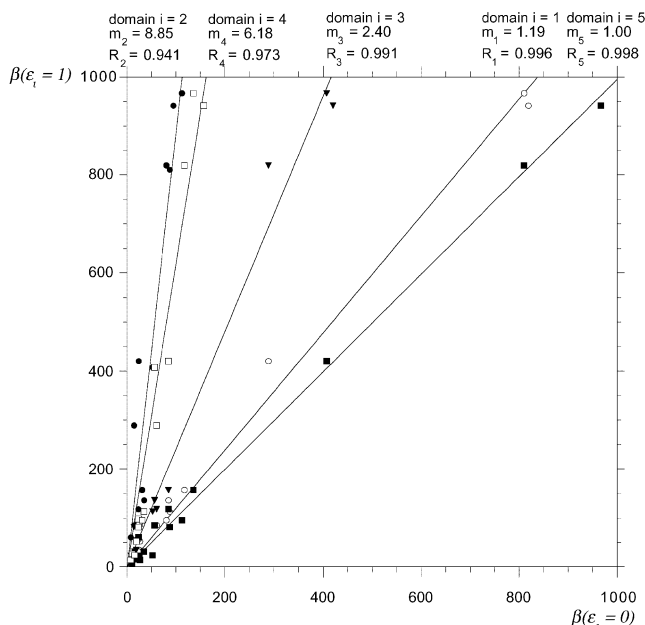


**Figure 1.** Plots of  $\beta(\epsilon_i = 1)$  (hyperpolarizability of structures with a carbomerized  $i$ th domain) versus  $\beta(\epsilon_i = 0)$  (hyperpolarizability of the corresponding structures with non-carbomerized  $i$ th domain) for each fixed domains  $i = 1-5$  defined in Scheme 1.  $\beta$  in  $10^{-30} \text{ cm}^5 \text{ esu}^{-1}$  units. Linear fits are monoparametric (passing through the origin). The  $m_i$  parameters are defined in the main text and eq 3.  $R_i$  denotes the correlation coefficient for the  $i$ th independent fit over the  $i$ th domain.

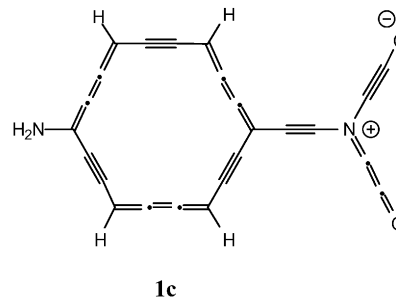
each domain, i.e., the  $\text{C}\equiv\text{C}$  bond linkages (1) and (3), the bridge (2), the acceptor (4), and the lateral  $\text{C}-\text{H}$  bonds (5). The correlation coefficients  $R_i$  are always greater than 0.94.<sup>21</sup> The greatest slope corresponds to the  $p$ -(carbo)phenylene bridge unit ( $m_2 = 8.85$ ), with the next one being that of the (carbo)nitro group ( $m_4 = 6.18$ ), followed by those of the bonds to the acceptor and to the donor ends ( $m_3 = 2.40$ ,  $m_1 = 1.19$ ). These variations suggest a multiplicative general formula (eq 3):

$$\beta = \beta^0 \prod_{i=1}^{i=4} [1 + (m_i - 1)\epsilon_i] \quad (3)$$

A one-parameter fit provides  $\beta^0 = 6.18 \times 10^{-30} \text{ cm}^5 \text{ esu}^{-1}$  which has the same order of magnitude (within the range 0–1000 for the considered  $\beta$  values) as the static hyperpolarizability of  $p$ -nitroaniline  $\beta(\mathbf{1a}) = 10.12 \times 10^{-30} \text{ cm}^5 \text{ esu}^{-1}$ . As anticipated in the framework of the two-level model, carbomerization of the  $\text{N}-\text{H}$  bonds of the donor group (domain 0) does not have a significant influence on the hyperpolarizability:  $941.3 \times 10^{-30} \text{ cm}^5 \text{ esu}^{-1} = \beta(\mathbf{1b}) \approx \beta(1111) = 967.0 \times 10^{-30} \text{ cm}^5 \text{ esu}^{-1}$ . Likewise, the negligible influence of the carbomerization of the lateral  $\text{C}-\text{H}$  bonds of the aromatic bridge (domain 5) has been verified (a fifth term to be included in (eq 3) is found  $m_5 \approx 0.995 \approx 1$ ). The assumed relevance of a four-digit description of a set of 16 main carbomer structures is a posteriori justified.

(21) Carbomerization of domains 1, 3, or 5 in structure  $e_1e_2e_3e_4e_5 = 01010$  affords aberrant points at the abscissa  $\beta = 97.33 \times 10^{-30} \text{ cm}^5 \text{ esu}^{-1}$  (the latters have been discarded for the linear regressions). Nevertheless, the aberrations are positive: the corresponding carbomerizations have a positive nonlinear effect, affording still higher  $\beta$  values:  $\beta(11010) = 407.3$ ,  $\beta(01110) = \beta(\mathbf{1c}) = 809.9$ ,  $\beta(01011) = 288.7$ .

## Scheme 2. Partial Carbomer Structure (0111) of **1a**, with an Optimal $\beta$ /Simplicity Ratio



Carbomerizations of both the skeleton of the  $p$ -phenylene bridge (domain 2) and the nitro group (domain 4) are thus essential. Carbomerization of the phenylene–nitro bond (domain 3) is generally twice as efficient as that of the phenylene–amino bond (domain 1) and is also essential to achieve very high  $\beta$  enhancement. This is illustrated in  $\mathbf{1c} = 0111$  (Scheme 2) that contains only three carbomerized domains (2, 3, and 4) and exhibits an 80 times greater  $\beta$  value:  $\beta(\mathbf{1c}) = 810 \times 10^{-30} \text{ cm}^5 \text{ esu}^{-1}$ .  $\mathbf{1c}$  is therefore an optimal compromise between synthetic feasibility and high  $\beta$  value.

The observed increase of  $\beta$  in the carbomeric species must be due to either a specific effect of the overall preservation of connectivity and symmetry in the carbomerization process or merely the well recognized effect of increasing the size of the conjugated bridge between the donor (one nitrogen atom) and the acceptor (two oxygen atoms). To bring out the specific effect of carbomerization, one defines the *specific molecular hyperpolarizability* as the ratio of  $\beta$  to the number  $N$  of non-hydrogen atoms of the structure:  $[\beta] = \beta/N$ . This quantity should reflect the actual NLO efficiency of a structure in view of future applications in material sciences: the smaller the  $N$  value, the smaller the molecular volume in the crystal,<sup>22</sup> and the higher the volumic bulk SHG efficiency  $\chi^{(2)}$  for a given crystal packing.<sup>23</sup> Table 1 shows that the relative specific molecular hyperpolarizability of  $\mathbf{1a}$  with respect to  $\mathbf{1b}$  and  $\mathbf{1c}$  is equal to 22 and 29, respectively. By comparison, an elongated version of PNA  $\mathbf{1a}$ , such as  $p$ -(dimethylamino)- $p$ -nitro-*trans*-stilbene (DANS) for which the conjugated bridge is roughly as long as the one in  $\mathbf{1c}$  (C11 versus C13), exhibits a specific hyperpolarizability enhanced by a factor of 3.5 only.<sup>6</sup>

In many practical applications, the NLO response is proportional to  $\beta$  but also to  $\mu$ , the dipole moment of the chromophore.<sup>24</sup> Therefore, the  $\mu\beta$  product is often referred to as a figure of merit for NLO chromophores. The specific NLO efficiency of a molecule within this approach can be measured by the quantity  $\mu[\beta] = \mu\beta/N$  (Table 1).

From  $\mathbf{1a}$  to  $\mathbf{1b}$  or  $\mathbf{1c}$ ,  $\mu\beta$  is multiplied ca. 200, whereas  $\beta$  is merely multiplied by ca. 100, and the same trend

(22) The non-hydrogen atomic density in molecular crystals is empirically found to be very close to a universal constant:  $1/18 \text{ \AA}^{-3}$ .  $[\beta]$  is proportional to the volumic molecular hyperpolarizability:  $\beta/(18N) \text{ esu \AA}^{-3}$ .

(23) Zyss J.; Oudar, J. L. *Phys. Rev. A* **1982**, *26*, 2028.

(24) Nalwa, H. S., Watanabe T., Miyata, S., Eds.; *Nonlinear Optics of Organic Molecules and Polymers*; CRC Press: Boca Raton, FL, 1997; Chapter 4.

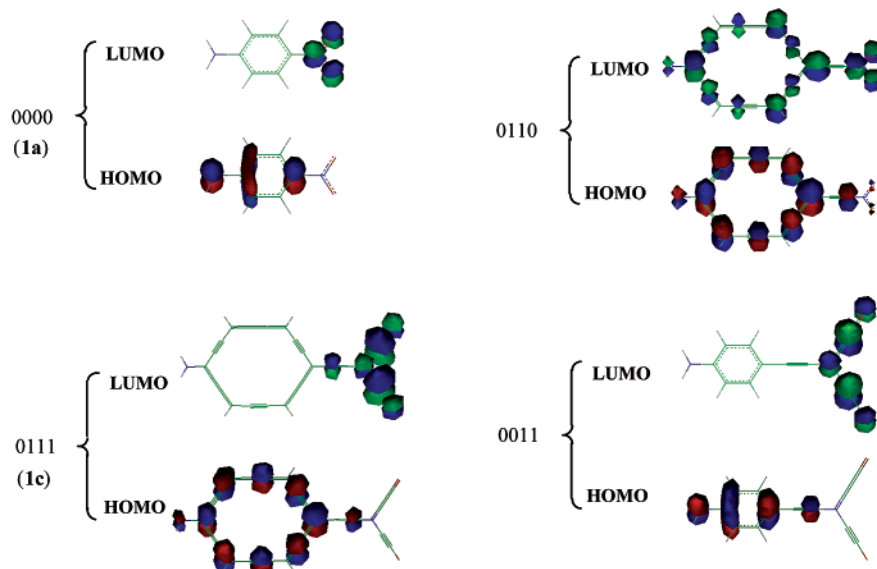


**Figure 2.** Localization of the HOMO and LUMO in **1a**, **1c**, and partial carbomers 0110 and 0011 with either the nitro group or the *p*-phenylene ring carbomerized.

**Table 2.** Transitions between the Ground State (**1**) and Main Excited States for the Four Partial Carbomers of *p*-Nitroaniline **1a**, All Having an Acetylene Connection between the Phenylene Domain and the Nitro Domain

com- pound $\epsilon_1\epsilon_2\epsilon_3\epsilon_4$	main tran- sitions	state % <sup>a</sup>	$\lambda_{\max}$ (nm)	$f$	$\Delta\mu$ (D)	composition of CI expansion <sup>b</sup>
0000 ( <b>1a</b> )	1 → 4	74.3	330	0.45	11.8	-0.973 $\chi_{26-27}$
0011	1 → 4	79.8	531	0.63	19.2	0.956 $\chi_{38-39}$
	1 → 5	13.9	470	1.06	2.89	0.973 $\chi_{37-39}$
0110	1 → 3	17.6	587	0.77	3.42	0.385 $\chi_{53-56}$ -0.895 $\chi_{54-55}$
	1 → 5	38.8	434	1.35	10.6	0.618 $\chi_{53-56}$ + 0.688 $\chi_{54-57}$
	1 → 8	22.1	385	1.78	6.54	0.753 $\chi_{53-55}$ -0.629 $\chi_{54-56}$
0111 ( <b>1c</b> )	1 → 4	85.6	809	1.51	19.2	0.964 $\chi_{62-63}$

<sup>a</sup> Contribution of the *i*th transition (state % =  $\beta_{g \rightarrow e(i)} / \sum_{j=1}^{j=300} \beta_{g \rightarrow e(j)}$ ) to the Calculated  $\beta_{2\text{Level}}$ . <sup>b</sup> Orbital 26 (27) is the HOMO (LUMO) for 0000, 38 (39) is the HOMO (LUMO) for 0011, 54 (55) is the HOMO (LUMO) for 0110, and 62 (63) is the HOMO (LUMO) for 0111.

is observed for  $\mu[\beta]$ : indeed, the carbomerization acts on both  $\beta$  and  $\mu$ . Within this approach, the theoretical benefit of the carbomerization of NLO chromophores is thus very suitable.

## Discussion

The relevance of the two-level model can be discussed on the basis of the transitions from which the NLO properties stem. Such an analysis has been performed for representative carbomer structures (Table 2). The two-level model appears to be a satisfactory approximation not only for *p*-nitroaniline but also for the 0111 (**1c**) and 0011 carbomer structures. In these cases, indeed, one transition (i.e., the HOMO → LUMO transition) accounts for more than 70% of the actual  $\beta$  value. However, this is not true anymore for the 0110 carbomer for which at least three transitions contribute to the NLO properties.

The semiempirical (ZINDO) HOMO and LUMO are depicted in Figure 2 for representative carbomer structures discussed above. The HOMO is expected to have strong weights on the donor part of the molecule,

**Table 3.** ZINDO-Computed  $\beta_0$  Values (in  $10^{-30} \text{ cm}^5 \text{ esu}^{-1}$  Units) for 16 Partial Carbomers of  $\text{NH}_2$ -(Bridge)- $\text{NO}_2$  Chromophores with Typical Bridges: *p*- $\text{C}_6\text{H}_4$ , *trans*- $\text{CH}=\text{CH}$ , and  $-\text{C}\equiv\text{C}-$ <sup>a</sup>

$\epsilon_1\epsilon_2\epsilon_3\epsilon_4$	<i>p</i> - $\text{C}_6\text{H}_4$	<i>trans</i> - $\text{CH}=\text{CH}$	$-\text{C}\equiv\text{C}-$
0000	10.12	4.47	4.76
0001	26.79	2.64	0.79
0010	25.15	14.54	15.55
0011	87.85	39.04	45.58
0100	7.89	10.88	15.55
0101	14.21	32.4	45.58
0110	23.16	29.47	15.55
0111	80.7	178.29	132.87
1000	23.09	14.76	15.55
1001	97.33	37.79	45.58
1010	85.12	28.68	15.55
1011	809.93	88	132.87
1100	60.24	20.93	15.55
1101	288.66	75.46	132.87
1110	117.56	59.26	34.32
1111	819.08	295.51	255.35
$m_1$	1.19 ( <i>R</i> = 0.996)	1.72 ( <i>R</i> = 0.981)	2.09 ( <i>R</i> = 0.942)
$m_2$	8.85 ( <i>R</i> = 0.941)	3.21 ( <i>R</i> = 0.942)	2.09 ( <i>R</i> = 0.942)
$m_3$	2.40 ( <i>R</i> = 0.991)	3.73 ( <i>R</i> = 0.935)	2.09 ( <i>R</i> = 0.942)
$m_4$	6.18 ( <i>R</i> = 0.973)	4.57 ( <i>R</i> = 0.946)	6.45 ( <i>R</i> = 0.832)

<sup>a</sup> These structures are denoted by  $\epsilon_1\epsilon_2\epsilon_3\epsilon_4$  sets, where  $\epsilon_i$  (=0, 1) indicates whether the domains *i* = 1, 2, 3, and 4 (analogous to those defined in Scheme 1) are carbomerized or not. The corresponding  $m_i$  factors were determined with one-parameter linear fits: correlation coefficient are given in brackets.

whereas the LUMO is expected to have strong weights on the acceptor part. In the most NLO-efficient carbomer **1c**, the HOMO and LUMO are well separated, whereas in the less efficient 0110 carbomer, they both have appreciable weights throughout the molecule. In structure **1c**, for example, because of the contribution of the inserted *sp* carbon atoms, the *p*-carbophenylene bridge acts as a good donor toward the carbonitro group, lowering the donor effect of the amino group.

The general process can be applied to other types of donors, bridges, and acceptors (Table 3). Beside the *p*-phenylene bridge detailed above, the *trans*-ethylene bridge  $-\text{CH}=\text{CH}-$ , and to a lesser extent the acetylene bridge  $-\text{C}\equiv\text{C}-$ , have been extensively used to improve the  $\beta$  value between (donor, acceptor) couples. The

## Scheme 3. Various Structures Obtained by Changing the Donor End in 1c

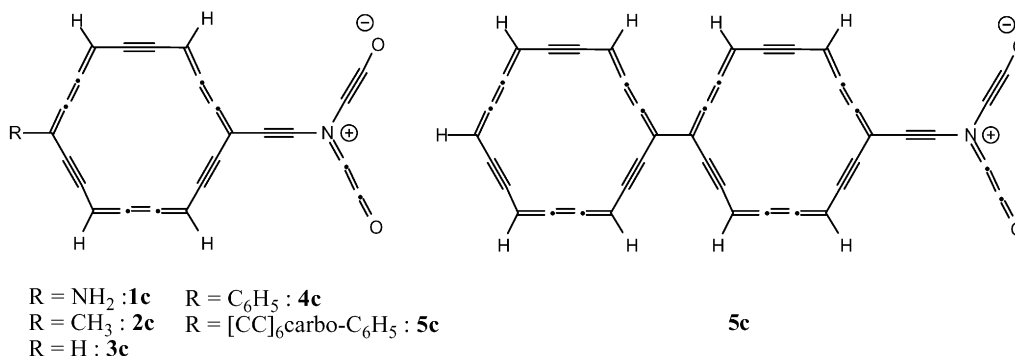


**Table 4. ZINDO-Computed  $\beta_0$  Values in  $10^{-30} \text{ cm}^5 \text{ esu}^{-1}$  Units for Various Derivatives of **1c** where the Donor End NH<sub>2</sub> Has Been Replaced by Various R Substituents**

entry	$\beta_0$	$N$	$ \beta /N$
<b>1c</b> (R = NH <sub>2</sub> )	941.28	28	33.61
<b>2c</b> (R = CH <sub>3</sub> )	695.58	28	24.84
<b>3c</b> (R = H)	633.07	27	23.45
<b>4c</b> (R = C <sub>6</sub> H <sub>5</sub> )	964.88	33	29.27
<b>5c</b> (R = [C <sub>6</sub> ]carboC <sub>6</sub> H <sub>5</sub> )	2315.34	45	51.45

exaltation factor  $m_i$  of the  $i$ th domain (defined similarly as in Scheme 1) has been determined by a linear fit restricted to the corresponding factor in (eq 3; Table 3).

The exaltation factor  $m_2$  of the bridge itself varies in a wider range from 8.85 for *p*-C<sub>6</sub>H<sub>4</sub>, to 3.21 for *trans*-CH=CH and 2.09 for C≡C. The  $m_1$ ,  $m_3$ , and  $m_4$  values corresponding to the H<sub>2</sub>N–C bond, C–NO<sub>2</sub> bond, and NO<sub>2</sub> group, respectively, also slightly depend on the nature of the bridge (Table 3). However, although the domains are not strictly independent from each others with respect to NLO effects, approximate transferable parameters can be estimated as  $m_1 \approx 1.5 \pm 0.5$ ,  $m_2 \approx 3 \pm 1$ , and  $m_4 \approx 5.5 \pm 1$ . This shows that the proposed modular analysis of the carbomerization effect has an empirical predictive value.

Retaining the optimized partial carbomerization of **1c** (with three carbomerized domains 2, 3, and 4), the carbomerization of accepting and donating groups other than NO<sub>2</sub> and NH<sub>2</sub> can naturally be envisioned. The previous observations that the donor strength of NH<sub>2</sub> is lowered through the carbophenylene bridge and that the *p*-phenylene itself acts as a donor toward NC<sub>4</sub>O<sub>2</sub> encouraged us to tentatively replace the amine substituent of **1c** by R = CH<sub>3</sub> (**2c**), H (**3c**), or Ph (**4c**) (Scheme 3). Unexpectedly, the NLO property of **1c** is qualitatively preserved even in the most simple molecule **3c** of low functionality (Table 4). As suggested by the HOMO of **1c** (Figure 2), the substitution of NH<sub>2</sub> by weakly donating groups (e.g., CH<sub>3</sub> or C<sub>6</sub>H<sub>5</sub>) does not affect significantly the charge-transfer process and, hence, the hyperpolarizabilities of the chromophores.

Though not known as a typical donor, the R = Ph substituent affords a slight  $\beta$  enhancement in **4c** with respect to R = NH<sub>2</sub> in **1c**. The phenyl ring was carbomerized in turn: the  $\beta$  value for **5c** (i.e., for R = [C,C]<sub>6</sub>C<sub>6</sub>H<sub>5</sub>) is more than twice as high as the  $\beta$  value for **1c** and **4c**.<sup>25</sup> Because  $N_{5c}/N_{1c} = 45/28 \approx 1.61$  only, the specific effect of carbomerization vs lengthening of

the conjugation pathway is thus measured by an enhancement of the specific hyperpolarizability  $|\beta|$  by a factor of ca. 1.25.

**Critical Evaluation of the Carbomerization Process for NLO Purposes.** (i) *Efficiency–Transparency Tradeoff.* As is well-known, the enhancement of the  $\pi$  conjugation unvariably leads to reduction of the transparency in a large frequency domain (e.g.,  $\lambda \approx 800$ – $900$  nm for the better NLO carbomers reported in the present study). Therefore, before being envisioned for an actual application, the important issue of efficiency–transparency has to be considered for these chromophores in the near-IR domain (1.3 and 1.5 micron), where many optoelectronic devices should be operating.<sup>26</sup> The UV–vis spectrum of **1c** has been calculated using the CAChe-interfaced ZINDO program.<sup>27</sup> Because of the width of the main absorption band at  $\lambda_{\text{max}} = 809$  nm, the molar extinction coefficient at  $\lambda = 1.550$  nm remains as high as  $\epsilon = 7 \text{ L mol}^{-1} \text{ cm}^{-1}$ . Nevertheless, the very high NLO response ( $\mu\beta \approx 18500$ ) might be sufficient to stray from standard conditions by working at lower chromophore concentration where the transparency would be acceptable.

(ii) *Stability.* The MM calculations used for the exploration of a large range of structures (32 partial carbomers) lead to the optimal structure **1c**. Finer insight into the structure of the NC<sub>4</sub>O<sub>2</sub> carbonitro group was gained by geometry optimization of HNC<sub>4</sub>O<sub>2</sub> at a higher level of calculations (B3PW91/6-31G\*). The NC<sub>4</sub>O<sub>2</sub> sequence is indeed experimentally unknown although it has been described as a bidentate ligand bounded to tungstene centers through oxygen and the triple C≡C bond.<sup>28</sup> In this complex, the NC<sub>2</sub>O sequence is bent, at least partly because of the metal coordination.

The linear arrangement of NC<sub>2</sub>O of the HNC<sub>4</sub>O<sub>2</sub> model **6** has been first constrained during geometry optimization at B3PW91/6-31G\*, yielding structure **6A** as a second-order saddle point (Figure 3). Distortion along the mode of the first imaginary frequency (93.89i cm<sup>-1</sup>) yields two local minima structures of C<sub>2v</sub> symmetry **6B** and **6C**, whereas the distortion along the mode of the second imaginary frequency (229.87i cm<sup>-1</sup>) yields the asymmetric structure **6D** which turns out to

(26) (a) *Silicon-Based Optoelectronics*, special issue of *MRS Bull.* **1998**, 23, 4. (b) *Erbium-Doped Fiber Amplifiers: Principles and Applications*, Desurvive, E., Ed.; John Wiley: New York, 1994.

(27) CAChe Scientific, release 3.9; Oxford Molecular Inc.: XXX, XXX, 1996.

(28) Chisholm, M. H.; Ho, D.; Huffman, J. C.; Marchant, N. S. *Organometallics* **1989**, 8, 1626.

(25) This also reads  $m_0(\text{Ph ring}) \approx 2$ , where  $m_0$  is exaltation factor of the domain 0 (here occupied by a phenyl group).



**Table 5. Total and Relative Energies of the Structures of HNC<sub>4</sub>O<sub>2</sub> 6A–D (Figure 3)**

compound	total energy B3PW91/6-31G** (au)	relative energy (kcal mol <sup>-1</sup> )	total energy HF/6-31G** (au)	relative energy (kcal mol <sup>-1</sup> )	total energy CASSCF/6-31G** (au)	relative energy (kcal mol <sup>-1</sup> )
<b>6A</b>	-357.90053	9.00				
<b>6B</b>	-357.91336	0.91	-356.01219	3.55	-356.05480	1.74
<b>6C</b>	-357.91375	0.67	-356.01511	1.72	-356.05511	1.59
<b>6D</b>	-357.91481	0.00	-356.01785	0.00	-356.05765	0.00

**Table 6. Comparison between Experimental<sup>10,29</sup> and Calculated (B3PW91/6-31G\*\*) Data for a Representative Carbobenzene Derivative, C<sub>18</sub>Ph<sub>6</sub>**

data	structural		UV <sup>a</sup> λ <sub>max</sub> (nm)	<sup>1</sup> H NMR <sup>b</sup> δ (ppm)
	Csp–Csp (Å)	Csp–Csp <sup>2</sup> (Å)		
expt	1.22(1)	1.39(1)	472 (CHCl <sub>3</sub> )	9.49 (o), 8.01 (m), 7.74 (p)
calcd	1.236	1.380	394 (vacuum)	10.56 (o), 8.18 (m), 7.78 (p)

<sup>a</sup> From ZINDO Calculations. <sup>b</sup> Within the framework of GIAO formalism, at the B3LYP/6-31+G\*\* level of calculation.

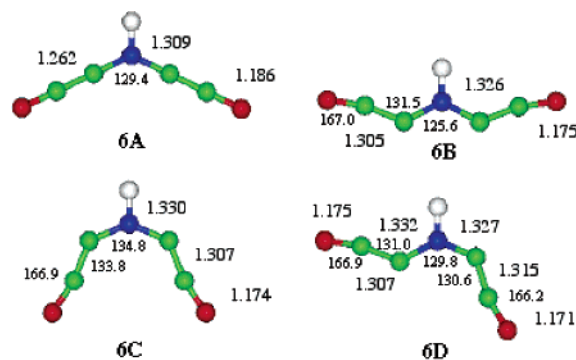


**Figure 3.** Optimized geometries **6A** (under the constraint of linear NC<sub>2</sub>O units) and **6B–6D** (no constraint) of HNC<sub>4</sub>O<sub>2</sub> at the B3PW91/6-31G\*\* level. Bond length are in angström units, and bond angles are in degrees.

be the global minimum (Figure 3; Table 5). However, **6B**, **6C**, and **6D** are very close in energy (Table 5). This DFT analysis of the HNC<sub>4</sub>O<sub>2</sub> fragment is in agreement with calculations performed at higher levels of theory such as MP2, CASSCF, and CI using a 6-31G\*\* basis (Table 5). It should be noted that all of these geometries are described as singlet states (quite well represented by single determinants), with the triplet state being at least 20 kcal/mol above (similar geometry as **6C**). Considering all of these facts and the zero-point vibrational motion (30 kcal/mol), it is difficult to conclude on the definitive geometry of the HNC<sub>4</sub>O<sub>2</sub> molecule. A dynamical analysis is required. Within an experimental prospect however, the structure **6A** is no more than 9 kcal/mol above several minima, and this small difference may be a priori neglected with respect the effects of H substitution, solvent polarity, and crystal packing. The linear NC<sub>2</sub>O arrangements of **6A** may thus be considered as a reasonable transferable structural feature of the NC<sub>4</sub>O<sub>2</sub> substituent: this a posteriori justifies its use to explore a large set of 32 partial carbomers, approximately but homogeneously treated by MM methods.

(iii) *Synthetic Feasibility.* The target molecule **1c** can be divided in two tricky components: the carbomeric phenylene ring and the carbomeric nitro group. Several examples of carbomeric benzene derivatives are now known.<sup>10,29</sup> The Ueda's synthesis of the hexaphenyl derivative C<sub>18</sub>Ph<sub>6</sub>, in 15 steps and 2% overall yield,<sup>10</sup> has been improved to 8 steps and 9% yield<sup>29</sup> and

extended to less substituted derivatives.<sup>29</sup> To validate our general calculation process, similar calculations have been performed for the representative example C<sub>18</sub>Ph<sub>6</sub>. As indicated in Table 6, the experimental–theoretical fit is excellent for structural and <sup>1</sup>H NMR data. The discrepancy (78 nm) obtained for the λ<sub>max</sub> value of the UV–vis spectrum is to be ascribed to solvatochromism. Indeed, the compound is violett-dark-red in the crystal state but gives orange-red chloroform solutions where the experimental spectrum has been recorded. As in the present calculation, our results on the PNA carbomers refer to an ideal solvent-free situation. Regarding the unknown carbomeric NC<sub>4</sub>O<sub>2</sub> unit, the present results suggests its synthesis as a novel challenge.

## Conclusion

Carbomerization expands structures by an “inflating” process instead of classical “lengthening” processes and modifies their characteristics everywhere at once. Regarding the variation of β in push–pull chromophores, the carbomerization approach thus appears as quite an alternative to Marder's approach which consists of sequential, though coupled, modifications of the donor, bridge and acceptor domains of the chromophores. At the MM-ZINDO level of theory, the approach appears to be, at least, relatively quite promising: β (respectively [β]) and μβ (respectively μ[β]) of structures **1c** and **5c** are predicted to be 80 (respectively 30) and 200 (respectively 70) times the respective values for PNA (**1a**). Though the numerical results could be fine-tuned at a higher level of theory, the structure **1c** is qualitatively optimized with respect to the foreseen β value/stability ratio. The carbomerization of the phenyl ring has been shown to be definitely possible.<sup>10,29</sup> By contrast, the process naturally lead to the unprecedented drawing of the carbonitro structure, NC<sub>4</sub>O<sub>2</sub>, and launches the challenge of its synthesis. Preliminary theoretical investigations have shown that this carbomer is not expected to have a classical behavior, especially owing to its extreme flexibility around the four formally *sp* carbon atoms.

**Acknowledgment.** The authors thank CALMIP (CALcul en Midi-Pyrénées, CICT-Toulouse-France) for computing facilities and Philippe Arnaud for computational assistance. R.C. also thanks the Ministère de l'Enseignement, de la Recherche et de la Technologie for ACIJ fundings.

CM0112993

(29) Sui-Seng, C.; Soleilhavoup, M.; Maurette, L.; Chauvin, R. unpublished results.